

The $uBVI$ Photometric System. II. Standard Stars

Michael H. Siegel¹ and Howard E. Bond²

*Space Telescope Science Institute, 3700 San Martin Drive, Baltimore, MD 21218;
msiegel@stsci.edu, bond@stsci.edu*

ABSTRACT

Paper I of this series described the design of a CCD-based photometric system that is optimized for ground-based measurements of the size of the Balmer discontinuity in stellar spectra. This “ $uBVI$ ” system combines the Thuan-Gunn u filter with the standard Johnson-Kron-Cousins BVI filters, and it can be used to discover luminous yellow supergiants in extragalactic systems and post-asymptotic-giant-branch stars in globular clusters and galactic halos. In the present paper we use $uBVI$ observations obtained on 54 nights with 0.9-m telescopes at Kitt Peak and Cerro Tololo to construct a catalog of standardized u magnitudes for standard stars taken from the 1992 catalog of Landolt. We describe the selection of our 14 Landolt fields, and give details of the photometric reductions, including red-leak and extinction corrections, transformation of all of the observations onto a common magnitude system, and establishment of the photometric zero point. We present a catalog of u magnitudes of 103 stars suitable for use as standards. We show that data obtained with other telescopes can be transformed to our standard system with better than 1% accuracy.

Subject headings: instrumentation: photometers — methods: data analysis — techniques: photometric — clusters (individual): M34, M41, M67 — stars: fundamental parameters

1. Introduction

Paper I in this series (Bond 2005) described the design of a new ground-based CCD photometric system which is highly optimized for measurement of the Balmer jump in stel-

¹Current address: University of Texas - McDonald Observatory, Austin, TX 78712; e-mail: siegel@astro.as.utexas.edu

²Visiting Astronomer, Kitt Peak National Observatory and Cerro Tololo Interamerican Observatory, National Optical Astronomy Observatory, which are operated by the Association of Universities for Research in Astronomy, Inc., under cooperative agreement with the National Science Foundation.

lar energy distributions. This “*uBVI*” system combines the *u* bandpass of Thuan & Gunn (1976) with the standard broad-band Johnson-Kron-Cousins *B*, *V*, and *I* filters. As shown in Paper I, the Thuan-Gunn *u* filter has a higher figure of merit for measuring the Balmer jump than the other commonly used ultraviolet filters (Strömgren *u*, the Sloan Digital Sky Survey *u'*, and Johnson *U*), because of its high throughput combined with little transmission longward of the Balmer discontinuity. The Johnson-Kron-Cousins filters were chosen at longer wavelengths because of the vast legacy of *BVI* stellar photometry, the broad bandpasses and high throughputs, and the extensive network of well-calibrated standard stars established through the work of Landolt and others.

The scientific motivation for a highly efficient filter system that measures the Balmer jump was presented in Paper I. To summarize, the most luminous stars in both young and old populations are objects of low surface gravities that have large Balmer discontinuities. In Population I many of the visually brightest non-transient stars are yellow supergiants of spectral types A, F, and early G, which can attain absolute magnitudes of $M_V \simeq -10$ (Humphreys 1983). The brightest stars of Population II are post-asymptotic-giant-branch (PAGB) stars that have left the tip of the AGB and are evolving through spectral types F and A at absolute magnitudes of $M_V \simeq -3.3$ (Bond 1997; Alves, Bond, & Onken 2001). Both classes of stars show considerable promise as tracers of their respective populations and as extragalactic standard candles.

Paper I presented a calibration of *uBVI* photometry against the basic stellar parameters of effective temperature, surface gravity, and metallicity, based on theoretical model stellar atmospheres. It was shown in that paper that the *u* – *B* color index is very sensitive to $\log g$ for stars with $T_{\text{eff}} \simeq 5,000$ to 10,000 K.

Proper exploitation of the system, however, requires a set of standard stars for the calibration of *uBVI* photometry. For *B*, *V*, and *I*, there is, of course, the widely used catalog of faint equatorial standards produced by Landolt (1992, hereafter L92).

Unfortunately, the Thuan-Gunn *u* band (hereafter referred to simply as “*u*”) did not share in this happy state of affairs at the beginning of the work described here. Thuan & Gunn (1976) provided a listing of *u* magnitudes in their system for over two dozen standard stars, but these stars are extremely bright for CCD work ($V \simeq 8$ –11), many of them are inaccessible from the southern hemisphere, and in general they are not as well calibrated in *BVI* as the L92 equatorial standards. To our knowledge, the initial photometric standards of Thuan & Gunn have only been augmented by Kent (1985), but again these stars are bright and many are accessible only from the north. Jørgensen (1994) established secondary standard stars for the Thuan-Gunn system, but omitted the *u* band. More recently, the SDSS ultraviolet filter (*u'*) has been extensively calibrated in the course of the SDSS survey, but of

course it is a different filter, with significant transmission above the Balmer jump and hence a lower figure of merit for measuring the size of the discontinuity (see Paper I for details). It was thus apparent that we would have to establish our own new and independent system of faint standard stars in the u band for calibration of our CCD-based $uBVI$ photometry.

Since we were using the standard BVI filters, we made the obvious decision to use standard stars from L92 to calibrate those three bandpasses. We therefore decided to base the u calibration on the same set of standard stars.

This paper describes the calibration process, and presents the list of standard u magnitudes for the L92 stars that resulted. §2 of this paper describes the observations and data reduction; §3 discusses the calibration of the measures to the BVI system; §4 describes the process of creating the catalog of standard u magnitudes; §5 presents the catalog of u magnitudes for the standard stars; §6 gives an example of the transformation of $uBVI$ photometry to our standard system; and §7 summarizes.

2. Standard-Star Observations and CCD Reductions

Our observational data consist of CCD $uBVI$ frames obtained with the 0.9-, 1.5-, and 4-m telescopes at Cerro Tololo Interamerican Observatory (CTIO), and the 0.9-, 2.1-, and 4-m telescopes at Kitt Peak National Observatory (KPNO), during a series of observing runs from 1994 through 2001. The primary aim of these runs was a large-scale search for PAGB stars in the halos of nearby galaxies and in Galactic globular clusters.

For purposes of calibration, Landolt fields selected from those listed in Table 1¹ were observed on every photometric night on which our program fields were observed. The fields listed in Table 1 were specifically chosen to contain several stars that lie within a few arcminutes of each other and are thus observable with a single CCD pointing. They also included at least one blue star, and the fields are distributed approximately uniformly around the celestial equator. We observed these fields intensively over an interval of seven years, and the u magnitudes have been reduced to a standard system as described in detail in this paper. The list of standard stars in these fields, presented below, now forms the basis for calibration of u -band photometry from any telescope in either hemisphere.

The majority of our data was taken with the 0.9-m telescopes at CTIO and KPNO, and therefore we will base the calibration of the $uBVI$ system on the observing runs from these two telescopes.

¹Finding charts, coordinates, and $UBVRI$ photometry for these stars can be found in L92.

On the CTIO 0.9-m, we used the 2048×2048 “Tek3” CCD. On the KPNO 0.9-m we used the 2048×2048 “T2KA” CCD. The fields of view for these two chips are $13' \times 13'$ for Tek3 at CTIO, and $23' \times 23'$ for T2KA at KPNO; the plate scales are $0''.396 \text{ pixel}^{-1}$ and $0''.688 \text{ pixel}^{-1}$, respectively. All of the u -band frames on both telescopes were obtained with a custom-built 4×4 -inch filter, described in detail in Paper I. For BVI , we used filter sets provided by KPNO and CTIO, with the following filter identifications: at CTIO: B-Tek2, V-Tek2, and I-KC31; at KPNO: 1569, 1421, 1444.

Table 2 gives details of the 15 0.9-m observing runs used for standardizing the $uBVI$ system. Columns 3 through 6 give the number of nights on which photometric observations of standard stars were obtained, the number of u -band CCD standard-star frames obtained during the run, the number of distinct standard stars observed during the run, and finally the total number of individual u magnitudes measured. Standard-star observations were made on 54 completely or partially photometric nights, on which 1075 CCD frames (271 of them in the u band) of Landolt fields were obtained, providing 1738 u -band measures of 142 potential standard stars.

We began the reductions by bias-subtracting, trimming, and flat-fielding all of the data frames using the standard IRAF² procedures in the *ccdproc* and *quadproc* packages. As noted in Paper I, the flat-fielding in the u band must be done using frames exposed on the twilight evening and morning sky; for B , V , and I we used both twilight and dome flats.

3. BVI Calibration

The first step in deriving the u standard system was the transformation of the BVI instrumental measures to the L92 system. Apart from being necessary to derive calibrated photometry for our program stars, this step allowed an independent check on the photometric quality of the observing nights.

Transformation of the BVI instrumental magnitudes began with the interactive identification of the L92 standard stars in each CCD field. We used the DAOPHOT package (Stetson 1987) to measure aperture photometry on each star for a series of apertures over a range of radii up to $14''$ for the CTIO data and $24''$ for the KPNO data (because of the larger

²IRAF is distributed by the National Optical Astronomy Observatory, which is operated by the Association of Universities for Research in Astronomy, Inc., under cooperative agreement with the National Science Foundation.

pixel scale).³ We did not subtract off neighboring stars before performing the multi-aperture photometry, because the standard system of L92, based on photoelectric aperture photometry, includes the light of any neighbors lying within the apertures. In practice, this choice has little noticeable effect since most of the chosen L92 standards lack nearby companions.

We used DAOGROW (Stetson 1990) to perform curve-of-growth analyses for each observing run. We did not, however, use aperture corrections for the standard stars, but instead used the total extrapolated magnitude measures produced by DAOGROW. We have found that these extrapolated magnitudes provide the best measures for standard-star calibration, since they measure nearly all of the light from each star, independently of small changes in seeing and focus. We have found that this method noticeably reduces the scatter in the photometric measurements.

In agreement with other authors (L92; Johnson & Bolte 1998) we found that two L92 “standards,” PG 1047+003C and PG 1323–086A, are low-amplitude variables, and we eliminated them at this stage. We also note that PG 1047+003 itself has been found to be a rapidly oscillating variable star (O’Donoghue et al. 1998), but given its small amplitude and short periods it remains usable as a photometric standard.

The final *BVI* photometric transformation equations were derived using the iterative technique described in Siegel et al. (2002). In this procedure, we do a simultaneous, interactive fit to the extinction, color, and zero-point terms via matrix inversion, through a code kindly provided by C. Palma. Airmass values were derived for each frame using the IRAF procedure *setairmass*, which calculates the photon-weighted airmass. We determined a single extinction coefficient in each filter for each observing run, and compensated for residual nightly variations in extinction by allowing the zero points to vary from night to night. Fixing the zero points and allowing the extinction coefficients to vary from night to night, which would have allowed for nightly variations, produced less internally consistent transformations and resulted in significant differences between photometry obtained on different nights.

In general, we were able to fit the L92 standard system to a precision of better than 0.01 mag. A handful of nights had slightly poorer transformations (but still with uncertainties ≤ 0.02 mag) because of slightly poorer observing conditions or a small number of observations. We found no need for non-linear extinction or color coefficients in *B*, *V*, and *I* during the calibration process.

³For the *u* magnitudes discussed below, we found that magnitudes were typically only usable out to radii of $\sim 5''$ because of the smaller stellar signals.

4. Creation of the u -Band Standard Magnitudes

Having reduced the BVI photometry for all of our standard-star observations and thereby having restricted ourselves to data obtained on demonstrably photometric nights, we turned to the establishment of a system of standard u magnitudes.

There are four steps in this process: (1) correction for the red leak in the u filter, (2) correction for atmospheric extinction, (3) unification of the outside-atmosphere u magnitudes from all of the observing runs on both telescopes onto a single consistent scale, and (4) adoption of a zero-point correction. Each of these steps is described in detail below.

4.1. Red Leak

As discussed in Paper I, the u filter has a small red leak at about 7100 Å. In the interest of maximizing throughput in the main ultraviolet band, and for maximum simplicity and economy, we made no attempt to block the red leak. Instead, we modeled it using the technical specifications of the cameras, filters, and detectors and model stellar atmospheres, as described in detail in Paper I. Since the red leak lies in the blue wing of the I bandpass, it is simplest to model the leak as a fraction of the I -band signal, with a small color term. The following corrections were calculated:

$$\text{RL}/I = 2.27 \times 10^{-4} - 6.80 \times 10^{-5}(B - V) + 5.36 \times 10^{-5}(B - V)^2 - 3.00 \times 10^{-5}(B - V)^3 \quad (1)$$

$$\text{RL}/I = 2.00 \times 10^{-4} - 6.26 \times 10^{-5}(B - V) + 5.23 \times 10^{-5}(B - V)^2 - 2.89 \times 10^{-5}(B - V)^3 \quad (2)$$

for the CTIO and KPNO 0.9-m telescopes, respectively. Here RL is the number of u electron counts from the red leak, I is the electron count measured in the I band, and $B - V$ is the color of the star on the standard system. All photon counts are per unit time and are measured inside the atmosphere. Therefore, the first step in the reductions was to subtract RL from the inside-atmosphere u electron counts, using either eq. 1 or 2.

The red-leak correction is of little practical importance in most applications, since the $uBVI$ system will usually be used for fairly blue stars; thus this step can usually be omitted. Nevertheless, we have included this correction in the reduction of the standard stars in order to improve the realism of the photometric system. As noted in Paper I, the red leak contributes about 1% of the total u signal for stars with $B - V = 0.8$, and rises to 10% of the signal at $B - V = 1.47$. We have eliminated from our standard-star catalog all stars with L92 $B - V$ colors redder than 1.45.

Our u -band standard-star observations usually had matching I -band observations, so that eqs. 1 or 2 could be applied. In a few cases, there was either no I image obtained

at the same time, or the corresponding I stellar image was saturated; these measures were discarded.

4.2. Atmospheric Extinction

The effects of atmospheric extinction were modeled in Paper I, where it was shown that because of the steep dependence of the extinction on wavelength across the u band, it is desirable to include both a small color term and a small non-linear airmass term in the extinction equation. The equation is thus

$$u_{\text{instr}}(X) = u_{\text{out}} + [a + b(B - V)]X + k_2X^2, \quad (3)$$

where $u_{\text{instr}}(X)$ is the instrumental u magnitude measured at airmass X , u_{out} is the u magnitude outside the atmosphere, $a + b(B - V)$ and k_2 are the linear and quadratic extinction coefficients, and $B - V$ is the stellar color on the standard system. In principle, all three coefficients could be fit directly if enough stars of a wide range of color were observed over a broad range of airmass.

In practice, we initially fixed b and k_2 to the theoretical values derived in the simulations of Paper I (-0.033 and -0.007 , respectively) and determined a directly for each observing run by intercomparing stars observed over a range of airmass. As noted in §3, we adopted an average a coefficient for each observing run; these ranged from 0.550 to 0.620 mag airmass $^{-1}$ over the duration of this project. The u extinction coefficients were found to be well-correlated with the extinction in the BVI filters.

After the initial solution for a , we intercompared the nights of each observing run to identify any night-to-night changes in photometric zero point. These changes were generally small (usually a few hundredths of a magnitude, but occasionally as large as 0.15 mag), and consistent with the previously derived zero-point shifts in the BVI calibration. We applied these zero-point corrections, then derived the extinction coefficients again, this time allowing both a and b to vary. The a terms were little changed from the initial solution, but there was a marked decrease in the scatter. The average b term was -0.0357 , in excellent agreement with the simulation. We iterated between nightly zero-point corrections and extinction corrections until all terms converged to 0.001 mag. We left k_2 fixed at the theoretical value since generally there were not enough observations of standard stars over a wide enough variety of airmasses for an empirical determination.

4.3. Unifying the Instrumental u -Band Photometry

The next step is to combine all of the u magnitudes from all of the observing runs into a catalog of standard values. It would be insufficient simply to average the instrumental outside-atmosphere u_{out} measurements over all of the different observing runs, for two reasons. (1) The CTIO and KPNO instrumental magnitudes were obtained with two different telescopes, cameras, and detectors, over intervals of several years; because of differences in the response functions, the instrumental u magnitudes from the two telescopes differ systematically (even though the same u filter was used at both telescopes). (2) Moreover, we empirically identified significant zero-point changes and small color shifts between data obtained during separate observing runs even with the same telescope, in both u and BVI . The latter systematic differences are likely the result of slight, possibly wavelength-dependent, variations over time in the throughputs of the telescope systems, and possibly long-term changes in atmospheric extinction and detector characteristics (including gain), or other more subtle effects.

We began the unification process by identifying the two observing runs that provided the best mutual agreement in u magnitudes. A statistical weight, W , was defined for each combination of two observing runs as $W = \sum 1/\sigma_i^2$, where σ_i is the standard deviation in the photometric measures of the i th star that the two runs have in common. The two runs whose comparison produced the greatest statistical weight were then combined.

The combination was done as follows. First, we calculated a transformation (zero point and color term) from one run to the other, using a least-squares fit of the form

$$u_1 = u_2 + c + d(B - V), \quad (4)$$

where u_1 and u_2 are the error-weighted average magnitudes in observing runs 1 and 2, respectively. This transformation was then applied in a weighted fashion to all of the magnitude measures in both observing runs as follows:

$$u'_1 = u_1 - [W_2/(W_1 + W_2)] [c + d(B - V)], \quad (5)$$

$$u'_2 = u_2 + [W_1/(W_1 + W_2)] [c + d(B - V)], \quad (6)$$

where the statistical weights of the individual observing runs were calculated from the scatter within each run using $W_1 = \sum 1/\sigma_{i,1}^2$ and $W_2 = \sum 1/\sigma_{i,2}^2$. These transformations placed both observing runs onto the same instrumental system, which is intermediate between the systems of the two runs. We then combined all of the measures to produce a new “observing run,” containing a weighted average of all of the stars in common, along with the transformed measures for the stars not in common.

This new “observing run” was then placed back into the set of observing runs, and the next-best pair of runs was identified. The process described above was repeated until all 15 runs had been incorporated.

The resulting catalog was then refined by re-determining the coefficients c and d that transform each of the 15 individual runs to the catalog of mean u magnitudes, and applying that transformation to all the individual magnitude measures. The purpose of this step was to put all of the independent measures on the same instrumental system in order to identify interactively any discrepant individual measurements (e.g., due to cosmic-ray hits, short-term atmospheric transparency variations, or other statistical fluctuations). These discrepant measures could only be recognized after an initial global solution had been made. We rejected 41 individual outliers.

We finally re-iterated the run-to-run solution by deriving a matrix-inversion fit of each run to the mean catalog, using the full transformation equation⁴ from Paper I,

$$u_{\text{instr}} = u_{\text{std}} + [a + b(B - V)]X + k_2X^2 + c + d(B - V). \quad (7)$$

The transformation color term, d , was now small, its largest departure from zero among all the runs being only -0.023 . The final magnitude measures for each star are the weighted averages of the transformed magnitudes.

As a check on the pipeline, we ran the B -band data through the same steps to determine if we could recover the L92 values. During the derivation, we reproduced measures of extinction, zero-point, and color terms that were close to those derived by simple matrix inversion in §4. When these terms were applied, the system was internally consistent to well within 1%. External comparison to the L92 values was worse but still within 1%. The slightly poorer external comparison is likely the result of our B filter being a poor match to Landolt’s, which produced strong color terms in the transformation (and opposite signs for KPNO and CTIO). When only CTIO data are considered, the external comparison is almost as good as the internal. The result shows that our pipeline produced an internally and externally consistent instrumental photometric system.

⁴Eq. 5 in Paper I also included a quadratic color term, $e(B - V)^2$, but this is necessary only when the measurements have not been corrected for red leak; see §6 below.

4.4. The Zero-Point Correction

The final step is to apply a zero-point correction to the catalog of mean outside-atmosphere u magnitudes of the standard stars. As discussed in Paper I, we will follow the precept adopted for the $uvby$ system by Strömgren (1963), who set the $u - b$ color of Vega and other A0 V stars to 1.0. Vega itself is, however, far too bright to observe with our equipment, and only a few of the L92 standards have colors in the vicinity of $B - V \simeq 0.0$. We therefore had to adopt an indirect approach to the zero point.

We observed three lightly reddened open clusters of near-solar metallicity: M34, M41, and M67. M34 was observed on 1997 September 20 with the KPNO 0.9-m telescope, M41 on 1995 October 16 with the CTIO 1.5-m, and M67 on 4 nights in 1998–99 with the KPNO 0.9-m. The u magnitudes of the cluster members were reduced to the instrumental system defined above, and the BVI magnitudes to the standard L92 system. The color indices were then adjusted for reddening, using the formulae in §4 of Paper I. Table 3 lists the three clusters and the adopted reddenings.

We then adjusted the zero point of the u magnitude system so that the dereddened $u - B$ colors of the main sequences of the three clusters would lie, on average, on the zero-age main-sequence (ZAMS) relation derived in §3.3 of Paper I from theoretical model atmospheres. We also gave some weight to fitting the color difference $(u - B) - (B - V)$ (the analog of the Strömgren c_1 index) to the theoretical ZAMS values (see Paper I), since the color difference has the advantage of placing the zero-point and reddening vectors nearly orthogonal to each other. (We also tried an experiment in which we fit *both* the color difference and the reddening, and successfully reproduced the $E(B - V)$ values of Table 3 to within 0.01 mag.)

Figure 1 shows the dereddened measurements for the three clusters, after application of the zero-point shift, superposed on the grid of theoretical colors for solar-metallicity stars calculated in Paper I. The overall agreement with the predicted shape of the ZAMS relation is good, although the scatter is somewhat higher for the redder stars (which are faint main-sequence stars with relatively large photometric errors in our short exposures; also, although we have removed obvious field stars, some field-star contamination remains).

M67 shows two characteristics worth noting in Figure 1. (1) Its main-sequence stars are slightly above the ZAMS relation, especially at $B - V \approx 0.5$ – 0.6 . These stars have already departed from the ZAMS because of the high age of M67, and are thus expected to have lower gravities than the ZAMS. (2) The bluer M67 stars are blue stragglers (ignored in adjusting the zero point for our u magnitudes). Figure 1 confirms that they have surface gravities similar to those of main-sequence stars, as was first demonstrated (based on Strömgren photometry) by Bond & Perry (1971).

5. The Standard Star Catalog

Our final catalog of standard stars for $uBVI$ photometry is presented in Table 4. We list all 103 stars for which we have five or more observations. The table gives the u magnitudes and $u - B$ colors, along with the mean errors of both quantities (derived from the internal scatter) and the number of u -band observations that were averaged. The V magnitudes and $B - V$ and $V - I$ colors of these stars are tabulated by L92.

The median mean error of our u magnitudes is 0.006 mag. Of the 103 standards, 97 have mean errors in u of less than 0.020 mag, and of these 69 have errors of less than 0.010 mag. Therefore, our catalog should easily provide calibrations to better than 1% accuracy.

In Figure 2 we plot the mean errors in the u magnitude vs. the magnitude. As expected, the errors increase with magnitude. If systematic errors remained in the system, we would expect a flattened distribution. We compared the mean errors with those output by DAOPHOT, and find that the mean errors are about 75% larger on average than expected from photon statistics. The larger discrepancies are actually for the brighter stars, for which the formal errors are almost entirely from photon statistics and are therefore small. This suggests that there is a small component of systematic error in our magnitudes, arising from such issues as flat-fielding, inadequately modeled red-leak corrections and photometric transformations, and short-term variations in atmospheric extinction. In addition, some of the stars may be low-amplitude variables. Nevertheless, as noted above, these errors are small for most of our standard stars, especially those with $u < 16$.

Figure 3 shows a $u - B$ vs. $B - V$ diagram for the standard stars listed in Table 4. The black symbols represent the standards from fields with galactic latitudes $|b| \geq 30^\circ$; red symbols mark those in the three low-latitude fields SA 98, Ru 149, and SA 110, which are likely to be reddened, along with those in the SA 95 region, which is overlain with $H\alpha$ emission and is thus also likely to be reddened. The figure confirms that these stars are indeed systematically more reddened than the high-latitude stars.

6. Sample Transformations

In this section we present a check of the precision of our $uBVI$ standard-star magnitudes, and give an example of calibration of data obtained with telescopes other than the CTIO and KPNO 0.9-m reflectors used to establish the standard stars.

The data to be transformed are from a 1995 October CTIO 1.5-m run, and a 1997 October KPNO 4-m run. The CTIO 1.5-m observations employed the identical Tek3 CCD

and u filter used for the CTIO 0.9-meter observing runs, but different B , V , and I filters. The KPNO 4-m observations, as compared with the KPNO 0.9-m, used a different CCD (T2KB), a different u filter (but of the same prescription), and different B , V , and I filters.

Our intention in constructing this system is that observers should be able to calibrate their observations to the $uBVI$ system without having to apply red-leak corrections and nonlinear extinction terms. Being able to apply these corrections would require detailed knowledge of the wavelength-dependent throughput of the telescope system being used, and such measurements are typically unavailable without significant effort (see also §5.3 of Paper I for further discussion). To test whether such a calibration will be possible, we made the transformations to our standard system using only linear and quadratic terms in color, and linear and color terms in airmass; thus, we are allowing these terms to absorb the effects of the red leak and the small quadratic extinction term. The transformation equation used is the same as eq. 12 of Paper I, except that k_2 is set to zero. We therefore have the following equation:

$$u_{\text{instr}} = u_{\text{std}} + [a + b(B - V)]X + c + d(B - V) + e(B - V)^2. \quad (8)$$

We solved this equation using the matrix inversion code and techniques described earlier (§3.2). Figure 4 shows the run of standard-star residuals for both transformed observing runs. The rms residuals for the u magnitudes for both runs are less than 1%, demonstrating excellent photometric consistency. Moreover, the u residuals are roughly comparable in size to the residuals of our BVI transformations for the same standard stars. Figure 4 does suggest a slight downturn at the faintest magnitudes. We have observed this trend in the BVI calibrations as well. It is probably the result of poor curve-of-growth extrapolation for the faintest stars (which also have large error bars from the photon statistics). We typically remove these faint stars from the calibrations, which still leaves a range of six magnitudes among the standards that are retained.

Our solutions for our entire data archive of 0.9-, 1.5- and 4-m runs at both CTIO and KPNO (with none of the data pre-corrected for red leak or extinction) produced transformations of similar or better quality. A typical transformation uses two color terms: linear color (i.e., d), and one of either the quadratic color coefficient (e) or the color term in extinction (b). Typical values of these coefficients are around ± 0.05 mag.

This exercise confirms that the effects of the red leak and non-linear extinction can be corrected for fully by using linear and quadratic color terms, as in eq. 8.

7. Conclusion

We have defined a CCD-based photometric system that combines the Thuan-Gunn u filter with the standard Johnson-Kron-Cousins BVI filters. In this paper we provide a catalog of u magnitudes for 103 standard stars that can be used (along with the BVI magnitudes given by L92) to calibrate observations taken through such filters. We have shown that our standard system can be reproduced using transformations of data from various telescope/detector systems to an accuracy of better than 1%.

Future papers will apply the $uBVI$ system to several programs involving searches for luminous stars in young and old stellar systems, and investigations of properties of the horizontal branch in globular clusters. We hope this paper will encourage other observers to use the $uBVI$ system for their own projects.

In addition to those thanked in Paper I, we are grateful to C. Palma for use of his calibration code and for help with adapting that code for the purposes of this study. We also thank C. Onken for helpful discussions. This work was supported in part by the NASA UV, Visible, and Gravitational Astrophysics Research and Analysis Program through grants NAG5-3912 and NAG5-6821.

REFERENCES

- Alves, D. R., Bond, H. E. & Onken, C. 2001, *AJ*, 121, 318
- Bond, H. E. 1997, in *The Extragalactic Distance Scale*, ed. M. Livio, M. Donahue, & N. Panagia (Cambridge: Cambridge University Press), 224
- Bond, H. E. 2005, submitted (Paper I)
- Bond, H. E. & Perry, C. L. 1971, *PASP*, 83, 638
- Harris, W. E., Fitzgerald, M. P. & Reed, B. C. 1981, *PASP*, 93, 507
- Harris, G. L. H., Fitzgerald, M. P. V., Mehta, S., & Reed, B. C. 1993, *AJ*, 106, 1533
- Humphreys, R.M. 1983, *ApJ*, 269, 335
- Johnson, J. A., & Bolte, M. 1998, *AJ*, 115, 693
- Jones, B. F. & Prosser, C. F. 1996, *AJ*, 111, 1193
- Jørgensen, I. 1994, *PASP*, 106, 967
- Kent, S. M., 1985, *PASP*, 97, 165

- Landolt, A. U. 1992, AJ, 104, 340 [L92]
- O’Donoghue, D., Koen, C., Lynas-Gray, A. E., Kilkenny, D., & van Wyk, F. 1998, MNRAS, 296, 306
- Siegel, M. H., Majewski, S. R., Reid, I. N. & Thompson, I. B. 2002, ApJ, 578, 151
- Stetson, P. B. 1987, PASP, 99, 191
- Stetson, P. B. 1990, PASP, 102, 932
- Strömngren, B. 1963, in Basic Astronomical Data, ed. K. Aa. Strand (Chicago: University of Chicago Press), 123
- Thuan, T. X., & Gunn, J. E. 1976, PASP, 88, 543
- Twarog, B. A., Ashman, K. M., & Anthony-Twarog, B. J. 1997, AJ, 114, 2556

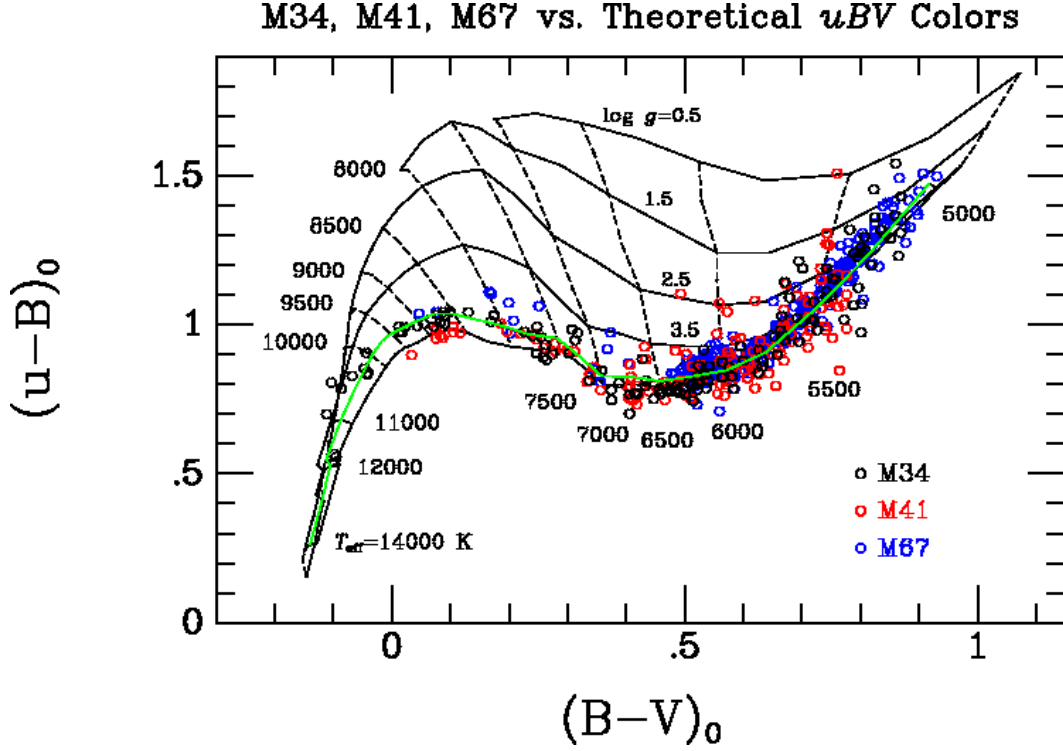


Fig. 1.— Dereddened $(u - B)_0$ vs. $(B - V)_0$ diagram for observations of three open clusters, M34 (black open circles), M41 (red open circles), and M67 (blue open circles). Adopted reddening values are given in Table 3. The grid of theoretical colors for $[\text{Fe}/\text{H}] = 0$ from Paper I is superposed in black, and the ZAMS relation from Paper I is shown as a green line. The zero-point of our u magnitude system was adjusted so that the main sequences of these three clusters would agree in the mean with the theoretical relation, whose zero-point is set such that Vega would have $u - B = 1.0$.

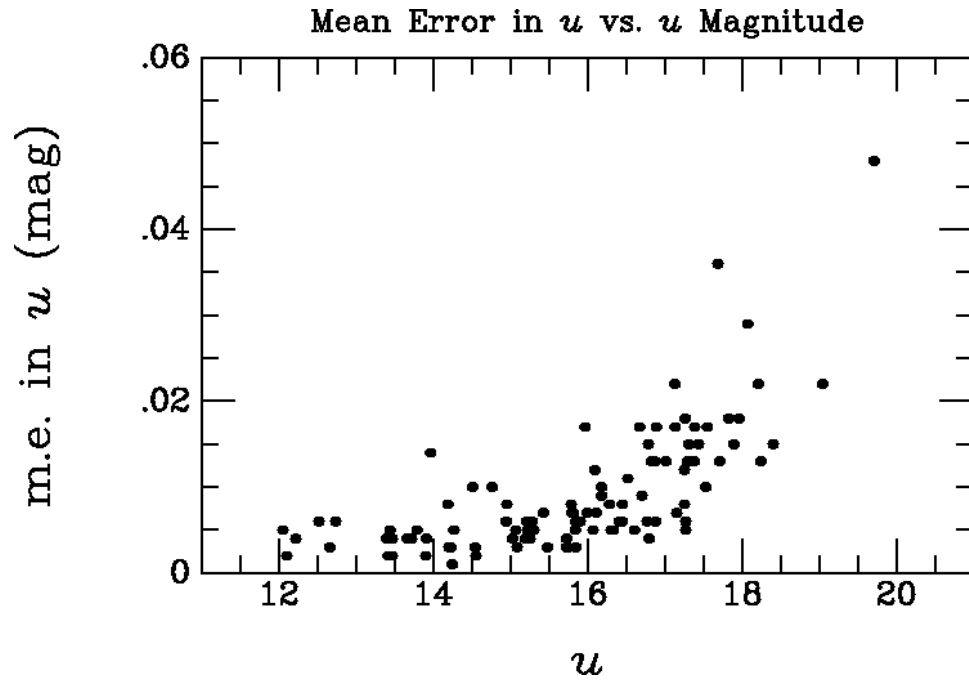


Fig. 2.— The run of standard errors of the mean (m.e.) against u magnitude for our $uBVI$ standard stars. Some of the high outliers may be low-amplitude variables.

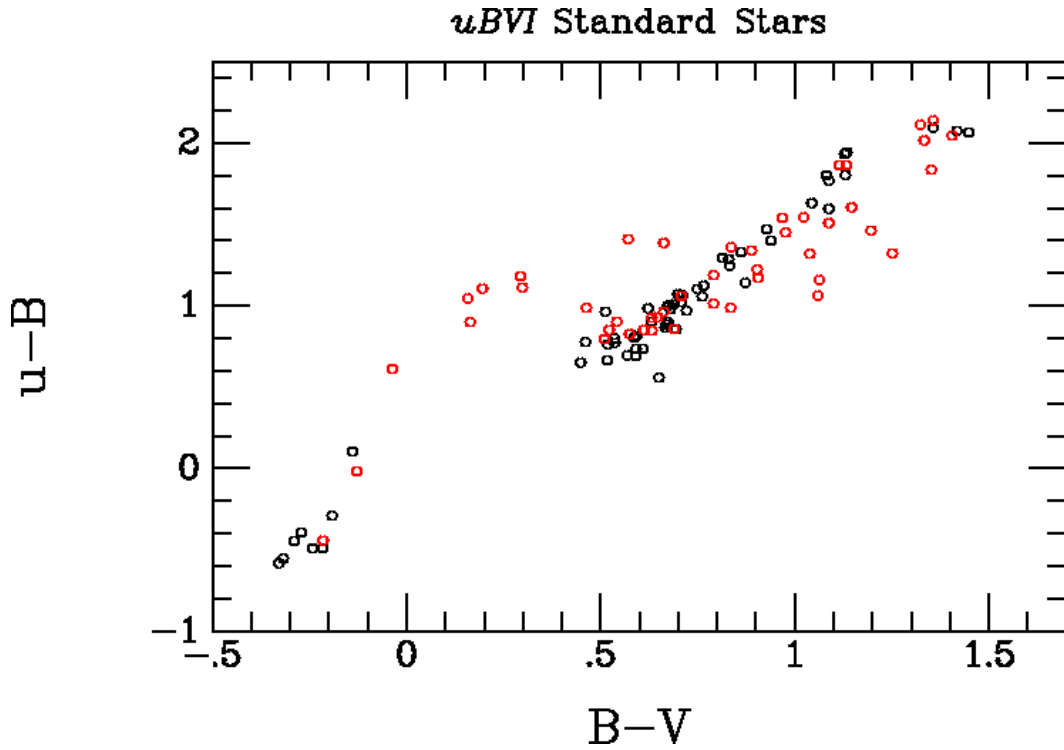


Fig. 3.— $u - B$ vs. $B - V$ diagram for the standard stars listed in Table 4. $B - V$ colors are taken from L92. Black open circles mark standards at high galactic latitudes ($|b| \geq 30^\circ$). Red open circles mark those in three low-latitude fields (SA 98, Ru 149, and SA 110) plus those in the reddened SA 95 region; note that these stars are systematically more reddened than the high-latitude stars.

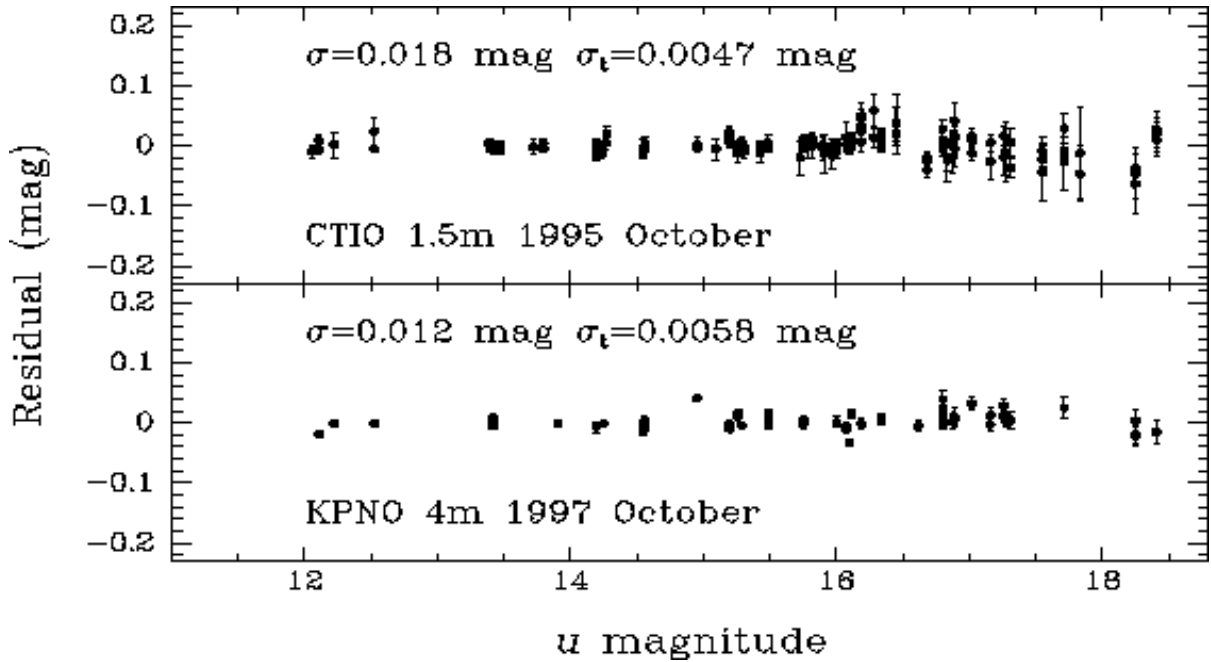


Fig. 4.— Transformation errors for two independent observing runs. Plotted are the residuals of the fits against u magnitudes of the standard stars. Given in the figure are both the unweighted scatter in the transformation residuals (σ), and the uncertainty of the transformation from the diagonal elements of the transformation matrix (σ_t) as defined in Harris, Fitzgerald, & Reed (1981).

Table 1. Standard Fields for *uBVI* Photometry

Field Name	RA (J2000)	Dec (J2000)	Galactic latitude, b ($^{\circ}$)
SA 92–249	00:54:34	+00:41:05	–62
PG 0231+051	02:33:36	+05:19:00	–49
SA 95–112	03:53:40	–00:01:13	–39
SA 98–650	06:52:05	–00:19:40	+0
Ru 149	07:24:15	–00:32:55	+7
PG 0918+029	09:21:32	+02:47:00	+34
PG 1047+003	10:50:09	–00:01:08	+50
SA 104–334	12:42:21	–00:40:28	+62
PG 1323–086	13:25:52	–08:50:15	+53
PG 1633+099	16:35:32	+09:47:04	+35
SA 110–362	18:42:48	+00:06:26	+2
Mark A	20:43:59	–10:46:42	–30
PG 2213–006	22:16:23	–00:21:45	–44
GD 246	23:12:20	+10:47:02	–45

Table 2. *uBVI* 0.9-m Observing Runs

Civil Dates	Telescope+Detector	N_{nights}	N_u frames	N_u std stars	N_u measures
1996 September 18–25	KPNO 0.9m+T2KA	4	16	38	96
1997 May 7–10	KPNO 0.9m+T2KA	2	12	31	55
1997 May 30–June 2	CTIO 0.9m+Tek3	2	11	21	59
1997 August 3–11	CTIO 0.9m+Tek3	7	29	45	162
1997 September 17–23	KPNO 0.9m+T2KA	4	20	33	94
1997 November 6–11	CTIO 0.9m+Tek3	5	25	62	151
1998 March 17–23	KPNO 0.9m+T2KA	2	11	34	71
1998 April 15–22	CTIO 0.9m+Tek3	4	23	43	110
1998 August 18–27	CTIO 0.9m+Tek3	8	42	71	224
1999 January 21–22	KPNO 0.9m+T2KA	1	10	42	73
1999 March 12–16	KPNO 0.9m+T2KA	3	16	57	132
1999 June 10–15	CTIO 0.9m+Tek3	2	11	22	49
1999 August 24–27	CTIO 0.9m+Tek3	3	14	32	73
2001 March 24–28	CTIO 0.9m+Tek3	3	16	26	67
2001 November 9–13	CTIO 0.9m+Tek3	4	15	50	133

Table 3. Open Clusters Used to Set the Zero Point

Cluster	$E(B - V)$	Reference
M34 (NGC 1039)	0.07	Jones & Prosser 1996
M41 (NGC 2287)	0.03	Harris et al. 1993
M67 (NGC 2682)	0.04	Twarog et al. 1997

Table 4. Catalog of $uBVI$ Standard Stars

Star	u	$u - B$	m.e.(u)	m.e.($u - B$)	n
SA 92–245	17.309	2.073	0.015	0.018	17
SA 92–248	18.405	1.931	0.015	0.034	18
SA 92–249	16.094	1.069	0.012	0.016	17
SA 92–250	15.284	1.292	0.006	0.008	17
SA 92–252	16.113	0.664	0.007	0.009	18
SA 92–253	17.018	1.802	0.013	0.015	17
SA 92–330	16.336	0.695	0.005	0.033	18
SA 92–335	14.194	0.999	0.008	0.009	18
SA 92–339	16.680	0.652	0.017	0.022	15
PG 0231+051	15.194	–0.582	0.004	0.012	27
PG 0231+051A	14.543	1.061	0.003	0.004	26
PG 0231+051B	18.247	2.064	0.013	0.015	27
PG 0231+051C	15.257	0.884	0.004	0.009	28
PG 0231+051D	16.884	1.769	0.006	0.010	28
PG 0231+051E	15.486	1.005	0.003	0.007	27
SA 95–41	16.186	1.223	0.009	0.009	19
SA 95–42	14.949	–0.442	0.006	0.011	18
SA 95–43	12.108	0.795	0.002	0.004	5
SA 95–97	16.895	1.171	0.017	0.028	5
SA 95–100	17.437	1.013	0.015	0.085	5
SA 95–105	16.001	1.451	0.007	0.007	19
SA 95–107	19.711	2.112	0.048	0.117	7
SA 95–106	17.710	1.322	0.013	0.063	18
SA 95–112	17.549	1.385	0.017	0.017	20
SA 95–115	16.874	1.358	0.013	0.013	13
SA 98–590	17.830	1.836	0.018	0.024	5
SA 98–614	17.897	1.160	0.015	0.065	5
SA 98–624	15.788	1.186	0.008	0.029	6
SA 98–626	18.209	2.045	0.022	0.023	6
SA 98–627	16.448	0.859	0.008	0.020	6
SA 98–634	16.184	0.929	0.010	0.012	6

Table 4—Continued

Star	u	$u - B$	m.e.(u)	m.e.($u - B$)	n
SA 98–642	17.269	1.408	0.018	0.052	6
SA 98–646	17.962	1.063	0.018	0.018	5
SA 98–650	13.474	1.046	0.002	0.003	6
SA 98–652	16.281	0.853	0.008	0.033	6
SA 98–666	13.795	0.899	0.005	0.007	6
SA 98–671	15.893	1.540	0.006	0.009	5
SA 98–670	15.425	2.139	0.007	0.007	6
SA 98–676	15.819	1.605	0.007	0.009	6
SA 98–682	15.306	0.925	0.005	0.008	6
SA 98–685	13.402	0.985	0.004	0.006	6
SA 98–688	14.230	1.183	0.003	0.005	6
SA 98–1002	15.966	0.824	0.017	0.019	5
SA 98–1082	16.830	0.985	0.013	0.020	5
Ru 149	13.721	–0.016	0.004	0.006	14
Ru 149A	15.906	1.113	0.006	0.010	14
Ru 149B	14.268	0.964	0.005	0.006	14
Ru 149C	15.727	1.107	0.003	0.008	14
Ru 149D	12.054	0.611	0.005	0.006	14
Ru 149E	15.091	0.851	0.003	0.008	14
Ru 149F	16.449	1.863	0.006	0.010	14
Ru 149G	14.272	0.902	0.005	0.007	14
PG 0918+029	12.663	–0.393	0.003	0.005	6
PG 0918+029A	15.799	0.773	0.007	0.010	6
PG 0918+029B	15.852	1.124	0.006	0.010	6
PG 0918+029C	15.070	0.902	0.005	0.006	6
PG 0918+029D	14.947	1.631	0.006	0.007	6
PG 1047+003	12.739	–0.445	0.006	0.008	18
PG 1047+003A	15.210	1.010	0.006	0.009	18
PG 1047+003B	16.409	0.979	0.006	0.012	17
SA 104–237	18.079	1.596	0.029	0.029	6
SA 104–239	17.388	2.096	0.017	0.020	11

Table 4—Continued

Star	u	$u - B$	m.e.(u)	m.e.($u - B$)	n
SA 104–244	17.292	0.691	0.013	0.017	10
SA 104–325	17.131	0.856	0.017	0.049	11
SA 104–330	16.707	0.817	0.009	0.031	11
SA 104–334	14.765	0.763	0.010	0.012	11
SA 104–336	16.521	1.287	0.011	0.015	11
SA 104–338	17.386	0.736	0.013	0.027	11
SA 104–339	17.535	1.244	0.010	0.010	10
SA 104–423	17.134	0.902	0.022	0.051	6
SA 104–444	14.953	0.964	0.008	0.013	6
SA 104–456	13.968	0.984	0.014	0.014	6
SA 104–L2	17.256	0.558	0.012	0.035	11
PG 1323–086	13.444	0.103	0.005	0.006	19
PG 1323–086C	15.730	1.020	0.004	0.006	19
PG 1323–086B	15.223	1.056	0.005	0.006	19
PG 1323–086D	13.474	0.807	0.004	0.005	18
PG 1633+099	13.914	–0.291	0.004	0.005	26
PG 1633+099A	17.270	1.141	0.006	0.008	24
PG 1633+099B	15.850	1.800	0.003	0.004	25
PG 1633+099C	16.307	1.944	0.005	0.006	26
PG 1633+099D	15.025	0.799	0.004	0.005	25
SA 110–266	14.248	1.341	0.001	0.003	26
SA 110–290	13.664	1.058	0.004	0.005	6
SA 110–349	17.691	1.508	0.036	0.036	6
SA 110–355	14.512	1.545	0.010	0.010	6
SA 110–358	16.787	1.318	0.015	0.015	6
SA 110–360	17.275	1.460	0.005	0.022	25
SA 110–361	13.904	0.847	0.002	0.004	26
SA 110–362	19.042	2.017	0.022	0.022	23
SA 110–364	16.613	1.865	0.005	0.009	26
Mark A	12.524	–0.492	0.006	0.006	23
Mark A1	17.256	0.736	0.008	0.012	23

Table 4—Continued

Star	u	$u - B$	m.e.(u)	m.e.($u - B$)	n
Mark A2	16.072	0.866	0.005	0.007	23
Mark A3	17.156	1.400	0.007	0.008	23
PG 2213–006	13.418	–0.489	0.002	0.004	35
PG 2213–006A	15.751	0.900	0.003	0.007	35
PG 2213–006B	14.558	1.103	0.002	0.003	35
PG 2213–006C	16.798	0.968	0.004	0.008	34
GD 246	12.221	–0.555	0.004	0.004	13
GD 246A	14.203	0.777	0.003	0.007	13
GD 246B	16.771	1.472	0.006	0.009	13
GD 246C	15.842	1.332	0.005	0.008	13